Coral Reefs
DOI 10.1007/s00338-016-1404-5

REPORT

Contrasting physiological plasticity in response to environmental stress within different cnidarians and their respective symbionts

Kenneth D. Hoadley[1] · Daniel. T. Pettay[1] · Danielle Dodge[1,2] · Mark E. Warner[1]

Received: 9 September 2015 /Accepted: 12 January 2016

Abstract Given concerns surrounding coral bleaching and ocean acidification, there is renewed interest in characterizing the physiological differences across the multiple host–algal symbiont combinations commonly found on coral reefs. Elevated temperature and CO_2 were used to compare physiological responses within the scleractinian corals *Montipora hirsuta* (*Symbiodinium C15*) and *Pocillopora damicornis* (*Symbiodinium D1*), as well as the corallimorph (a non-calcifying anthozoan closely related to scleractinians) *Discosoma nummiforme* (*Symbiodinium C3*). Several physiological proxies were affected more by temperature than CO_2, including photochemistry, algal number and cellular chlorophyll *a*. Marked differences in symbiont number, chlorophyll and volume contributed to distinctive patterns of chlorophyll absorption among these animals. In contrast, carbon fixation either did not change or increased under elevated temperature. Also, the rate of photosynthetically fixed carbon translocated to each host did not change, and the percent of carbon translocated to the host increased in the corallimorph. Comparing all data revealed a significant negative correlation between photosynthetic rate and symbiont density that corroborates previous hypotheses about carbon limitation in these symbioses. The ratio of symbiont-normalized photosynthetic rate relative to the rate of symbiont-normalized carbon translocation (P:T) was compared in these organisms as well as the anemone, *Exaiptasia pallida* hosting *Symbiodinium minutum*, and revealed a P:T close to unity (*D. nummiforme*) to a range of 2.0–4.5, with the lowest carbon translocation in the sea anemone. Major differences in the thermal responses across these organisms provide further evidence of a range of acclimation potential and physiological plasticity that highlights the need for continued study of these symbioses across a larger group of host taxa.

Keywords Temperature and CO_2 acclimation · Package effect · Chlorophyll *a* · Carbon limitation

Introduction

The genus *Symbiodinium* represents a highly diverse group of dinoflagellates well known for forming unique symbioses with several marine invertebrate taxa, including cnidarians, mollusks and sponges (Fitt 1985; Hoegh-Guldberg and Bruno 2010; Weisz et al. 2010). Through phylogenetic analysis of several genes, *Symbiodinium* are commonly divided into nine major clades (LaJeunesse 2001; Coffroth and Santos 2005). Recent attention has been placed on comparing this genetic diversity with physiological differences and tolerance to environmental stress. Coral bleaching, which describes the expulsion of symbionts from the host tissue, is a frequent and often fatal phenomenon most commonly associated with high-temperature stress (Brown 1997). In addition, stress brought on by changes in pH and carbonate chemistry due to ocean acidification is also of concern with respect to coral reef health (Brading et al. 2011; Comeau et al. 2013). With

Communicated by Biology Editor Dr. Simon Davy

Electronic supplementary material The online version of this article (doi:10.1007/s00338-016-1404-5) contains supplementary material, which is available to authorized users.

& Kenneth D. Hoadley
khoadley@udel.edu

1 School of Marine Science and Policy, University of Delaware, Lewes, DE, USA

2 Present Address: Harbor Branch Oceanographic Institute, Florida Atlantic University, Fort Pierce, FL, USA

major increases in sea surface temperature and pCO_2 predicted by the end of this century (IPCC 2013), understanding the physiological differences among host/*Symbiodinium* combinations and how they possibly mitigate stress related to climate change will become increasingly important in predicting the success of these organisms (Baker 2003).

Much *Symbiodinium* research has focused on scleractinian coral species due to their importance in calcium carbonate deposition and reef growth. However, non-calcifying symbiotic cnidarians also provide critical ecological functions, making their response to environmental change also of importance (Tkachenko et al. 2007). Recent, disturbance-induced phase shifts from calcifying scleractinians to non-calcifying anthozoans are one example (Tkachenko et al. 2007; Norstro¨m et al. 2009; Dudgeon et al. 2010) and highlight this possibility in response to high temperature and or elevated pCO_2. The growth rates and productivity of the anemone, *Anemonia viridis* increased with proximity to naturally occurring CO_2 seeps off the coast of Italy (Suggett et al. 2012) and numerous laboratory experiments have now documented the benefits of elevated pCO_2 for different anemone species (Towanda and Thuesen 2012; Gibbin and Davy 2014). In contrast, scleractinian studies have documented a much broader range of effects on calcification, respiration and photosynthesis (Kaniewska et al. 2012; Comeau et al. 2013; Edmunds et al. 2013; Schoepf et al. 2013). Reductions in scleractinian coral coverage due to thermal bleaching and ocean acidification, along with documented pCO_2 benefits to anemones, suggest that future corals reefs could be dominated by non-calcifying species. Nevertheless, additional research on other non-calcifying anthozoans is needed. For example, taxonomically, corallimorphs are rooted within the scleractinian lineage, making them an ideal (yet understudied) group of cnidarians for comparison with calcifying coral species (Medina et al. 2006; Kitahara et al. 2014). Understanding how different cnidarian symbioses respond to environmental stressors, including increased temperature and elevated pCO_2, may be a critical factor in predicting what cnidarian species dominate future coral reefs. Importantly, given that future reefs will likely encounter both elevated temperature and pCO_2 (Hughes and Connell 1999; Hughes et al. 2003; Hoegh-Guldberg et al. 2007), understanding their possible antagonistic or synergistic effects, and whether this varies across anthozoans, is of high importance.

For scleractinian corals, the efficiency of capturing solar radiation for photosynthesis is increased through light scattering by the skeleton (Enriquez et al. 2005; Wangpraseurt et al. 2012). Although these bio-optical properties result in highly efficient light capture, drawbacks exist. Reductions in symbiont densities from thermal bleaching dramatically increase the internal light field for remaining symbionts, potentially increasing the possible damage to the photosynthetic apparatus, resulting in a negative feedback for light capture efficiency (Rodriguez-Roma´n et al. 2006; Wangpraseurt et al. 2012). In contrast, the bio-optical properties of symbionts in non-calcifying symbiotic anthozoans likely differ and may significantly alter their photophysiological response to thermal stress and the light environment (Kuguru et al. 2010).

Changes in algal cell size and chlorophyll concentration can also be critical in managing environmental stressors such as high solar irradiance, allowing the symbiont to acclimatize to varying conditions so as to optimize productivity (Warner et al. 1996; Fitt et al. 2001; Key et al. 2010). However, the degree of plasticity can vary widely among different symbiont types and within different host species and taxa (Leal et al. 2015). The potential for physiological variability both among and within specific groups of *Symbiodinium*, along with differences in cnidarian host morphologies, significantly expands the array of possible acclimation and stress mitigation strategies for coping with climate change (Cooper et al. 2011; Leal et al. 2015).

Variable rates of autotrophic carbon uptake and translocation have been observed, suggesting that the specific host–symbiont combinations play an important role in establishing rates of carbon incorporation in these symbioses (Davy et al. 1996; Engebretson and Muller-Parker 1999; Davy and Cook 2001; Leal et al. 2015). Understanding differences in carbon incorporation among anthozoan species and how environmental stress affects them may be critical to our understanding of future reefs and their symbiotic constituents. However, characterizing symbiont productivity across coral species can be somewhat complex due to species-specific differences among host organisms. Better comparative metrics are needed to understand differences across host taxa.

The goal of this study was to use high-temperature and elevated CO_2 conditions to characterize physiological plasticity across three different host–symbiont combinations representing two different host taxa (Scleractinia and Corallimorpharia) in order to highlight physical features that are most important in responding to environmental stress within each holobiont. Bio-optical and biophysical differences among symbiont types were considered, along with how holobiont physiology might influence the symbionts' response/acclimation to environmental stress. When compared among species, our data set highlights a distinct inverse relationship between productivity and cell density, in agreement with previously established hypothesis regarding carbon limitation within the host. Rates of photosynthesis cell^{-1} to translocation cell^{-1} (P:T) are compared across species and discussed in reference to environmental stress.

Materials and methods

Experimental setup

Two scleractinian species, *Montipora hirsuta* and *Pocillopora damicornis*, were obtained from a commercial coral mariculture facility in New Albany, Ohio (Reef Systems Coral Farm), where the corals were held for over 10 yr. Individual nubbins were originally harvested from a single adult colony 1–2 yr prior to transportation to Lewes, Delaware. Once in Delaware, coral nubbins were allowed to acclimate for an additional 10 months prior to experimentation. Several individuals of the corallimorph, *Discosoma nummiforme* were purchased from a local aquarium shop and maintained under laboratory conditions for over 3 yr prior to experimentation such that the samples used in this study were second- or third-generation specimens. As the organisms used in this experiment represent clonal copies or fragments originally isolated from a single colony, our results cannot be used to infer population-wide trends. Rather, similar to other published physiological comparisons (Shick and Dowse 1985; Shick et al. 2011), our design appropriately highlights the degree of variation and acclimation within an individual colony as it pertains to changes in temperature and pCO_2, while minimizing experimental variability.

All samples were maintained in seawater collected from the Indian River Inlet, DE, during incoming tides. Seawater was filtered to 1 μm and UV sterilized prior to use. Typical seawater parameters after filtration were: temperature = 27 ± 0.5 °C, salinity = 33 ± 0.58, pH = 8.17 ± 0.05, total alkalinity = 2072 ± 47 μmol kg . All coral specimens were illuminated by a customized LED array (Cree XPG-R5, cool white; 5000–8300 K). To better simulate a natural diel light cycle, lights were ramped up from a minimum of 10 μmol quanta $_m^{-2}$ s^{-1} to a maximum of 400 μmol quanta $_m^{-2}$ s^{-1} over a 3-h period, then remained at 400 μmol quanta $_m^{-2}$ s^{-1} for 6 h, prior to ramping back down over the last 3 h within the 12:12 light/dark cycle.

Treatments consisted of two temperatures (26.5 and 31.5 °C) and two pCO_2 conditions (400 and 800 μatm) for a total of four separate treatment conditions. Corals were exposed to treatment conditions for a total of 18 d. Ambient and elevated pCO_2 conditions were maintained via a pH stat system, which controlled the bubbling of air, CO_2-free air and/or CO_2 into each treatment system based on the pH of the seawater. Temperature was maintained using electronically controlled titanium heaters housed in each sump (Neptune Systems). Within the high-temperature treatments, temperature was ramped 0.5 °C d from a starting temperature of 26.5 °C, until reaching the target of 31.5 °C. Each treatment system consisted of five 15-L aquaria connected to a central 416-L recirculating sump. Flow rates within each aquarium were held at 567 L h . A 40 % water change was preformed on each system every second day. Salinity was maintained at 32 ppt through daily top-offs with reverse osmosis and deionized (RO/DI) filtered water.

The pH stat microelectrodes (Ross Ultra Semi-Micro pH Electrode) were recalibrated every second day with NBS buffer standards and confirmed through independent measurements of pH (Fischer Scientific A815 Plus pH meter). Temperature was monitored electronically every 5 min (Neptune Systems) and salinity monitored every second day with a refractometer. Total alkalinity (TA) within each system was measured every 6 d using a bromocresol blue-based colorimetric assay with a fiber optic spectrometer (USB4000, Ocean Optics) and titrator (876 Dosimat plus; Yao and Byrne 1998). Accuracy of TA measurements was checked against a seawater standard (Scripps) and typically deviated by less than 5 %. Seawater chemistry parameters are shown in Table 1 and average temperatures for each treatment system are in Electronic Supplementary Material, ESM Fig. S1.

Symbiodinium identity

Symbiont genotypes were identified for each nubbin at the end of the experiment through amplification of the internal transcribed spacer 2 region (ITS2) of the ribosomal array and subsequently analyzed by previously published protocols for denaturing gradient gel electrophoresis (DGGE) and cycle sequencing (LaJeunesse et al. 2003).

Symbiont photochemistry and spectral absorbance

Maximum quantum yield of photosystem II (PSII, Fv/Fm) and the functional absorption cross section of PSII (σ_{PSII}) were measured using a fluorescence induction and relaxation (FIRe) fluorometer (Satlantic Inc, Halifax) on the final night of the experiment. Measurements were taken 1 h after the start of the dark period and consisted of five iterations of a 120-μs single turnover flash and analyzed by fitting each fluorescence transient curve using the *FIREPRO* software (Kolber and Falkowski 1998; Hennige et al. 2011).

PSII electron transport rates (ETR) were also measured on the last day. All measurements were first dark-acclimated for 30 min and then exposed to an actinic light source (Cree XPG-R5, cool white; 5000–8300 K, 354 μmol quanta m s) for 4 min. Electron transport rates were calculated as

$$ETR = \sigma^{'}_{PSII} \times \frac{F^{'}_{q}}{F^{'}_{m}} \times PFD \times 21{:}683$$

Table 1 Average conditions (mean ± SE) for each of the treatments

Temperature (°C)	Ambient CO_2		High CO_2	
	Ambient	Elevated	Ambient	Elevated
pH	8.15 ± 0.027	8.16 ± 0.034	7.91 ± 0.101	7.86 ± 0.062
pCO_2 (µatm)	376 ± 11.23	381 ± 2.48	850 ± 27.19	812 ± 22.98
TA (µmol kg^{-1})	2074 ± 69.67	2070 ± 113.17	2158 ± 13.62	2107 ± 16.13
Aragonite saturation Ω_a	3.04 ± 0.12	2.99 ± 0.02	1.83 ± 0.04	1.82 ± 0.05
Salinity (ppt)	33.21 ± 0.81	32.93 ± 0.61	33.50 ± 0.50	33.07 ± 0.18

All seawater carbonate chemistry based on pH (NBS) and total alkalinity (TA) measurements were calculated using the CO2SYS program (Lewis and Wallace 1998)

where σ_{PSII} = is the functional cross section of PSII measured under actinic light, F_q'/F_m' = effective quantum yield, PFD = photon flux density (354 µmol quanta m^{-2} s^{-1}) and 21.683 converts seconds to hours, µmol e to mol e and A^{*2} quantum to m mol RCII (RCII = PSII reaction center; Suggett et al. 2003).

Spectral absorbance measurements were performed as described in Enriquez et al. (2005) with reflectance (R) measured using a spectrometer (USB2000, Ocean Optics) and absorbance (A) calculated as $A = \log[1/R]$. Bleached skeletons were used as blanks for 100 % reflectance for the scleractinian corals, whereas a spectralon reflectance standard functioned as the blank for the corallimorphs. Irradiance was provided by a full-spectrum halogen light source (KL2500 LCD, Schott). A running average was used to smooth data. Because we were only interested in chlorophyll *a* absorption, only the chlorophyll peak (675 nm) was tested for significant differences among treatments.

Photosynthetic carbon assimilation and translocation

Coral nubbins were placed in separate 7 mL scintillation vials containing 4 mL of seawater spiked with 15 µL of ^{14}C-labeled bicarbonate (specific activity 17 µCi µmol). Six nubbins per treatment were used for each coral species. Due to their size, *D. nummiforme* were placed in 20 mL vials containing 10 mL of spiked seawater with the same concentration of ^{14}C-labeled bicarbonate. Vials were placed on a LED light-table (Cool White Cree XPG-R5; 600 µmol photons m^{-2} s^{-1}; 28 °C) for 90 min. A higher light intensity was used during the incubation to ensure all samples were at maximum photosynthesis, and preliminary tests ensured that no signs of photoinhibition were evident (data not shown). An additional six nubbins from each species and treatment were placed in vials with ^{14}C-spiked seawater and held in the dark for 90 min to account for carbon uptake in the dark. Three additional vials containing only the spiked seawater were also included for measurement of total activity.

After ^{14}C incubations, a 400-µL sample of seawater was removed from each vial for calculation of total labeled organic carbon (TOC) released by the holobiont. For *P. damicornis* and *M. hirsuta*, nubbins were then removed from the spiked seawater and placed into a 1 mol L HCl in seawater solution for less than 2 h to dissolve the skeleton. The remaining tissue was then homogenized in 1 mL of seawater using a tissue homogenizer (Tissue tearor, Biospec). For *D. nummiforme*, each specimen was removed from the spiked seawater and ground in 6 mL of seawater. The resulting homogenate was centrifuged (5000 *g*) for 5 min to separate the host and symbiont portions. A 500 µL (1 mL for *D. nummiforme*) subsample was removed and used to measure carbon translocated to the host (H_s), while 100 µL of the remaining supernatant was used for calculating host protein content. The remaining algal cell pellet was resuspended in 500 µL of filtered seawater (FSW, 1 mL for *D. nummiforme*), vortexed and then centrifuged again to extract any remaining host supernatant (RH_s) from the algal pellet. The resulting algal pellet (S) was then resuspended a final time in 400 µL of FSW. All samples measured for radioactivity were acidified with an equal volume of 0.1 mol L^{-1} HCl, placed in 7 mL scintillation vials for 24 h and then combined with 5 mL of scintillation cocktail (Ultima Gold, Perkin Elmer) prior to reading with a liquid scintillation counter (Beckman LS-6500). All measurements and calculations follow established methods for *Exaiptasia pallida* (Davy and Cook 2001). Translocation (T_L) and photosynthesis $_{(Pnet)}$ rates were determined by the average specific activity (g C dpm) and the duration of the incubation. The fraction of carbon translocated (T_L) was calculated as

$$T_L = TOC + H_s + RH_s$$

and then normalized to host protein. TOC is the total organic carbon, while H_s and RH_s are the host supernatant and remaining host supernatant, respectively.

Net photosynthesis $_{(Pnet)}$ was normalized to total algal cells and calculated as

$$P_{net} = TOC + H_s + RH_s + S$$

where S is the algal pellet described above. Using the ratio

of the above equations, the fraction of photosynthate translocated to the host was calculated as

$$T_L = P_{net} = (TOC + H_s + RH_s) = (TOC + H_s + RH_s + S)$$

Cell density and chlorophyll samples (200 µL each) were removed from the initial homogenized sample of the animal prior to centrifugation for ^{14}C analysis. Algal cell density and volume were assessed by replicate hemocytometer counts ($n = 6$) under 1000× magnification. Samples were photographed using a Nikon microphot-FXA epifluorescent microscope and then analyzed by computer using Image J software (NIH). For photopigment quantification, pelleted cells were lysed in 90 % methanol with a bead beater (BioSpec) for 60 s, incubated at −20 °C for 2 h and then centrifuged for 5 min at 5000 rpm to remove remaining debris. Chlorophyll *a* concentration was then calculated using established protocols (Porra et al. 1989). Host protein concentrations were measured by the BCA method (Thermo Scientific), with bovine serum albumin used for standards. All absorbance measurements (chlorophyll and protein) were performed with a plate reader (FLUOstar Omega BMG labtech).

Photosynthesis:translocation ratio

Photosynthetic activity was compared directly to translocation by plotting symbiont-normalized maximal photosynthetic rates against symbiont-normalized translocation rates. This analysis also included data from an earlier study with an additional non-calcifying symbiotic anthozoan, the anemone *E. pallida*, which hosted three different genotypes of *S. minutum*. These additional data originated from a similar experiment, using the same treatment system and methods as this study, with anemones exposed to pCO_2 levels of 400 and 800 µatm for 1 month at 26.5 °C (Hoadley et al. 2015).

Statistical analysis

Individual variables were tested for assumptions of homogeneity of variance and normality of distribution using the Levene and Shapiro–Wilk tests, respectively. If either test invalidated these assumptions, the data were square-rooted or log-transformed prior to further analysis. A two-way analysis of variance (ANOVA) was used to test for significant main effects of pCO_2 and temperature and any potential interactive effects between the two ($\alpha = 0.05$). When interaction effects were found, a Tukey post hoc test was performed to test for differences among the four treatments. If data failed to meet assumptions of normality, a Kruskal–Wallis test with multiple comparisons was used instead. Nonlinear and linear regressions were used to describe the relationships between net photosynthesis and symbiont density or total translocation.

Associations among all of the physiological variables measured were examined by a principal components analysis (PCA). Variables were normalized to remove potential error from differences in unit scale associated with the different physiological measurements included in the analysis. Only principal components (PC) with eigenvalues greater than one were retained in the analysis. Significant correlations with each principal component for the 11 variables are provided in Table 2. All statistical analyses used the open source software R with 'car' and 'pgirmess' and 'FactoMineR' packages installed (http://www.R-project.org) or with Prizm 6 (GraphPad Software).

Results

Symbiont identification and stability

A subset of each species was genotyped prior to the start of the experiment. Only one dominant symbiont type was detected in each sample. Specifically, *Symbiodinium C3* was found in *D. nummiforme*, *C15* in *M. hirsuta* and *D1* in *P. damicornis*. In addition, each symbiosis remained stable throughout the experiment, with no additional algal types detected within the different treatments.

Photochemistry

There was a significant interaction with temperature and pCO_2 for the *C3* symbiont ($P = 0.0016$) as Fv/Fm declined with increasing temperature. However, the decline was significantly less under high pCO_2 (Table 2). An interactive effect was also observed for the *D1* symbiont ($P = 0.0011$) as Fv/Fm significantly increased with temperature under both pCO_2 treatments. Fv/Fm yields also significantly increased with CO_2 but only at ambient temperature (Table 2). No significant differences were observed within the *C15* symbiont.

The electron transport rate significantly declined with elevated temperature within the *C3* ($P = 0.0297$) and *D1* ($P = 0.0277$) symbionts, whereas no change occurred for the *C15* symbiont (Fig. 1; ESM Table S1). Likewise, the functional absorption cross section $_{(6PSII)}$ did not change significantly in the *C15* symbiont, but significantly decreased with temperature ($P = 0.0040$) in *Symbiodinium D1* (Table 3). In addition, there was a significant interactive effect of temperature and pCO_2 ($P = 0.0059$) within the *C3* symbiont as σ_{PSII} increased with temperature within the low but not elevated pCO_2 treatments (Table 3).

Table 2 Mean (±SE) maximum quantum yield of PSII (Fv/Fm) for *Discosoma nummiforme*, *Montipora hirsuta* and *Pocillopora damicornis* ($n = 6$). ANOVA column presents results from two-way ANOVA with main effects temperature (temp) and pCO_2 (CO_2). *LT* low temp, *HT* high temp, *HTHC* high temperature, high pCO_2 treatment, *HTLC* high temperature, low pCO_2 treatment, *LTHC* low temperature, high pCO_2 treatment, *LTLC* low temperature, low pCO_2 treatment, *NS* no significant results

Temperature (°C)	Ambient CO_2		High CO_2		ANOVA results	Tukey post hoc results
	Ambient	Elevated	Ambient	Elevated		
(*C3*) *D. nummiforme*	0.338 ± 0.011	0.173 ± 0.011	0.323 ± 0.019	0.256 ± 0.012	Temp*CO_2, $P = 0.002$	LT > HT; HTLC < HTHC
(*C15*) *M. hirsuta*	0.204 ± 0.005	0.211 ± 0.009	0.227 ± 0.009	0.218 ± 0.013	NS	
(*D1*) *P. damicornis*	0.267 ± 0.002	0.348 ± 0.004	0.301 ± 0.007	0.336 ± 0.005	Temp*CO_2, $P = 0.0001$	LT < HT; LTLC < LTHC

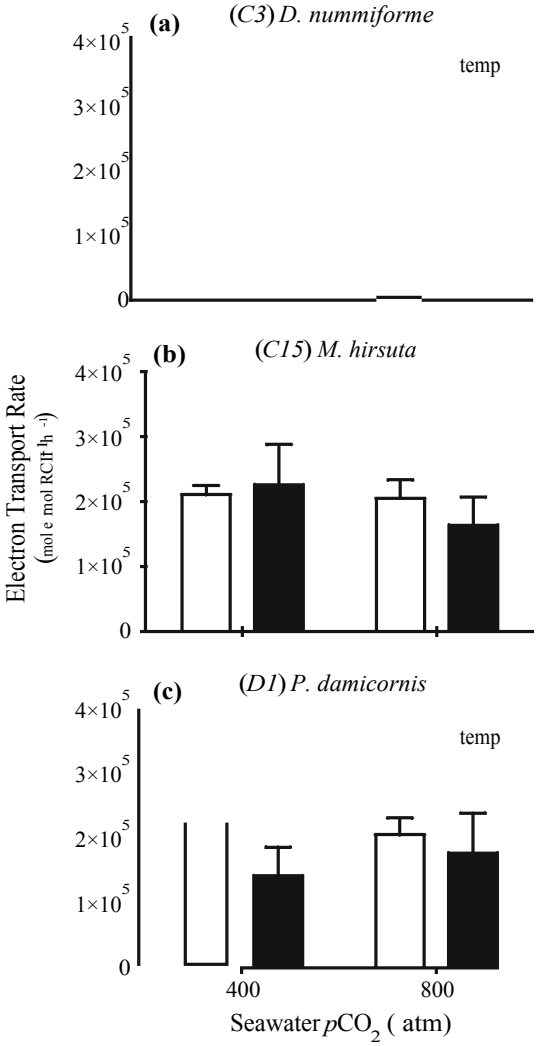

Fig. 1 Electron transport rates for *Discosoma nummiforme* (a), *Montipora hirsuta* (b), *Pocillopora damicornis* (c). Averages plus standard error are shown for two pCO_2 levels and two temperatures (26.5 °C: *open bars*, 32 °C: *dark bars*). The designation 'temp' indicates a significant temperature effect (two-way ANOVA)

Symbiodinium physiology

Chlorophyll concentration cell^{-1} significantly declined with temperature for *Symbiodinium C3* ($P < 0.0001$) and *D1* ($P = 0.0140$), while it increased significantly ($P = 0.0150$) for *C15* (Fig. 2a–c; ESM Table S3). Although *C3* density did not change, a significant temperature-induced decline occurred in the *C15* symbiont ($P = 0.0212$; Fig. 2d, e; ESM Table S3). A significant interactive effect for temperature and pCO_2 was observed for *Symbiodinium D1* ($P = 0.0198$), as cell density significantly declined with temperature within the ambient treatment but not within the elevated pCO_2 treatments (Fig. 2f; ESM Table S3). Cell volume also did not change significantly within *Symbiodinium C3*, whereas cell volume increased with temperature for *C15* ($P = 0.0042$; Fig. 2g, h; ESM Table S3). A significant interactive effect for the *D1* symbiont volume ($P = 0.0068$) was observed, as cell volume increased significantly with elevated temperature but only at ambient pCO_2 (Fig. 2i; ESM Table S3). Cellular chlorophyll density (pg Chla μm^{-3}) decreased with temperature ($P < 0.0001$) in the *C3* symbiont (Fig. 2j, Table S3). Although no significant changes were observed within *C15* cells, an interactive effect ($P = 0.0093$) was noted for *D1* symbionts with cellular chlorophyll density decreasing with temperature under ambient but not elevated pCO_2 conditions (Fig. 2k, l; ESM Table S3).

Although there was no significant difference in colony light absorption in the corallimorph, elevated temperature resulted in a significant increase in absorbance in *M. hirsuta* ($P = 0.0002$; Fig. 3a, b; ESM Table S3). In contrast, an interactive effect was observed for *P. damicornis* ($P < 0.0001$) where absorbance decreased with temperature within the low, but not elevated pCO_2 treatment. In addition, absorbance in the elevated pCO_2 treatments was significantly lower

Table 3 Mean (±SE) functional absorption cross section of PSII (A^{*2} quantum $^{-1}$, $n = 6$) for *Discosoma nummiforme*, *Montipora hirsuta* and *Pocillopora damicornis*. ANOVA column presents results from two-way ANOVA with main effects temperature (temp) and pCO_2 (CO_2). *HTHC* high temperature, high pCO_2 treatment, *HTLC* high temperature, low pCO_2 treatment, *LTHC* low temperature, high pCO_2 treatment, *LTLC* low temperature, low pCO_2 treatment, *NS* no significant results

Temp. (°C)	Ambient CO_2		High CO_2		ANOVA	Post hoc test
	Ambient	Elevated	Ambient	Elevated		
(*C3*) *D. nummiforme*	379 ± 13	726 ± 76	403 ± 16	480 ± 24	Temp*CO_2 $P = 0.00594$	HTLC [HTHC; LTLC \ HTLC
(*C15*) *M. hirsuta*	477 ± 17	498 ± 23	472 ± 34	418 ± 28	NS	
(*D1*) *P. damicornis*	421 ± 21	351 ± 11	401 ± 10	371 ± 16	Temp $P = 0.004$	

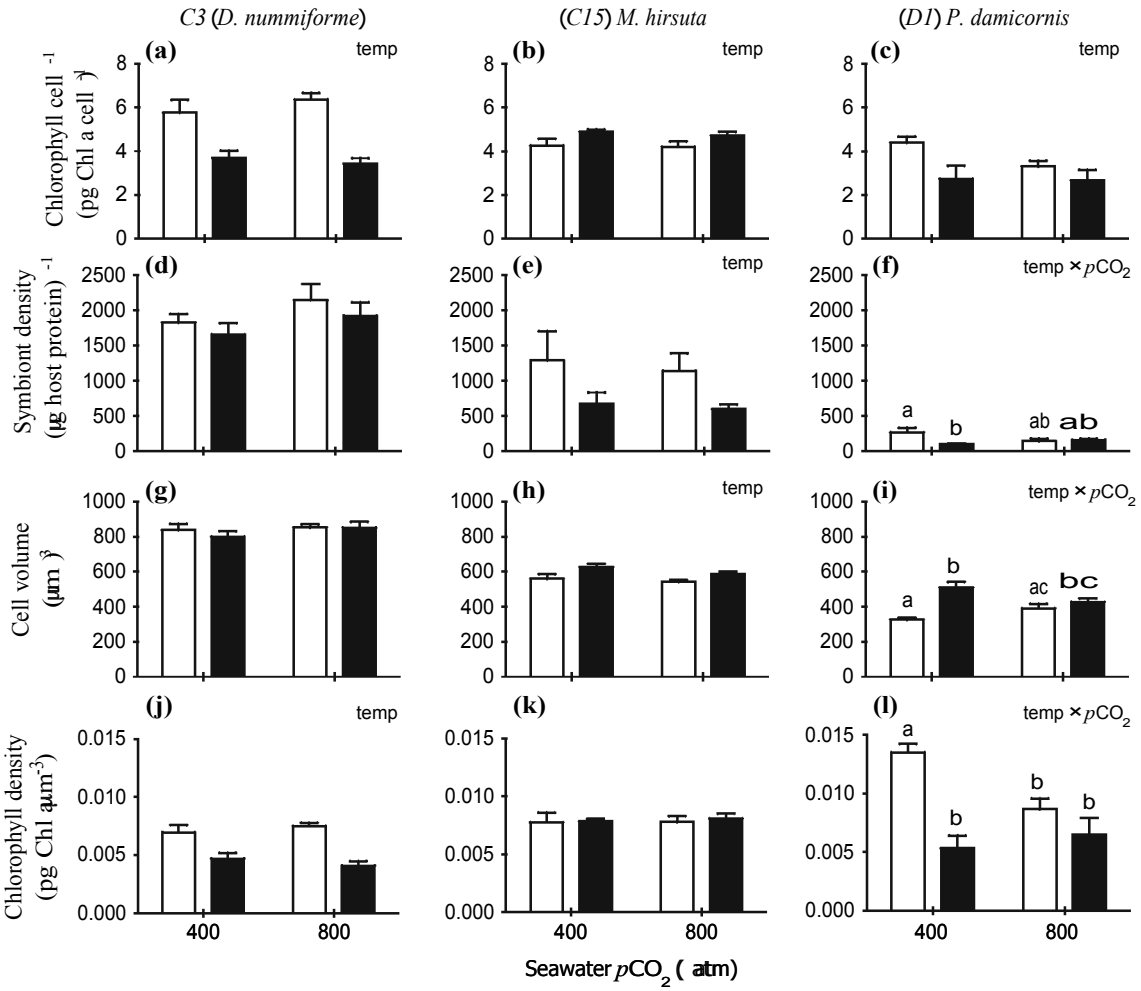

Fig. 2 Chlorophyll *a* content per cell, cell density, cell volume and chlorophyll density for *Discosoma nummiforme* (a, d, g, j), *Montipora hirsuta* (b, e, h, k) and *Pocillopora damicornis* (c, f, i, l). Averages plus standard error ($n = 6$) are shown for two pCO_2 levels and two temperatures (26.5 °C: *open bars*, 32 °C: *dark bars*). The designations 'temp' and 'temp × pCO_2' indicate significant temperature or interactive effects (two-way ANOVA). The *letters above each bar* indicate the results of Tukey pairwise analysis for significant interactions

than the ambient pCO_2 and ambient temperature treatment but significantly higher than the combined ambient pCO_2 and elevated temperature treatment (Fig. 3c; ESM Table S2).

Carbon uptake and translocation

Although no significant differences in net photosynthesis were noted for *D. nummiforme*, net photosynthesis

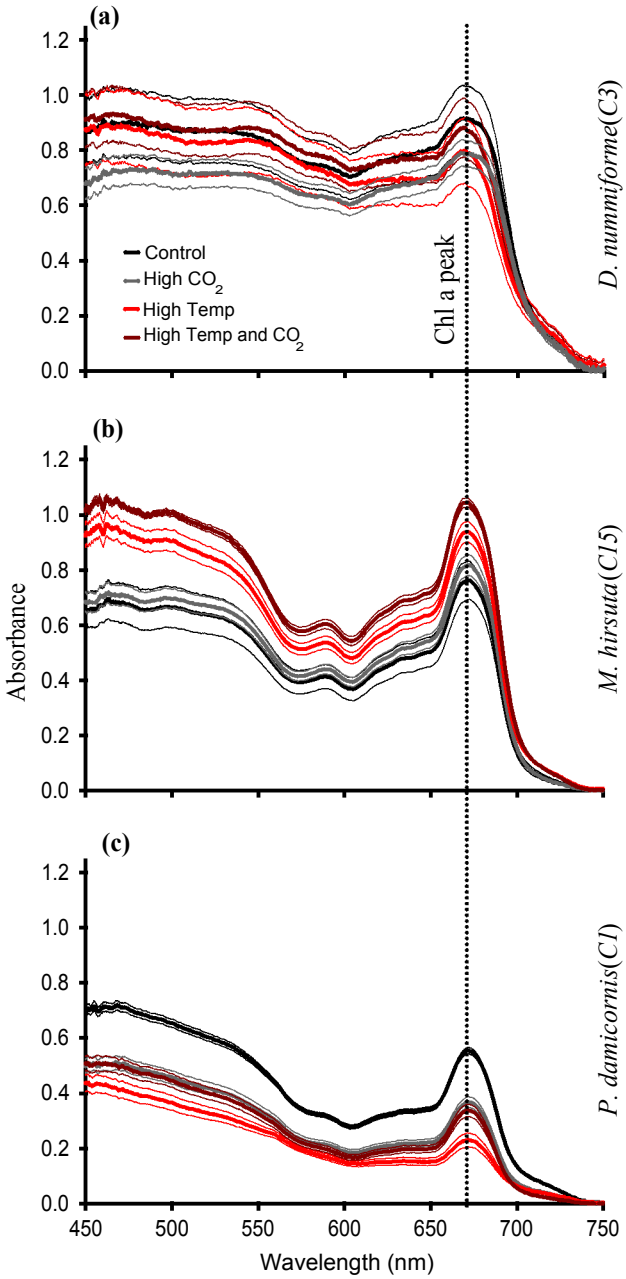

Fig. 3 Spectral absorbance profiles for *Discosoma nummiforme* (a), *Montipora hirsuta* (b) and *Pocillopora damicornis* (c). *Lines* represent the mean (*heavy line*) ± standard error (*light line*) for each treatment. The *black line* signifies ambient temperature and CO_2. *Gray* is ambient temperature and elevated CO_2. *Red* is high temperature at ambient CO_2, and *maroon* is high temperature and high CO_2. The *dotted vertical line* signifies peak absorbance for chlorophyll *a* (675 nm)

increased with elevated temperature in *M. hirsuta* ($P < 0.0001$) and *P. damicornis* ($P = 0.0104$; Fig. 4a–c; ESM Table S4). When viewed from the host perspective (as g carbon translocated g host protein^{-1}), there were no significant changes in translocation rates (Fig. 4d–f; ESM Table S4). The fraction of photosynthate translocated to the host did not change significantly with treatment type for *M. hirsuta* or *P. damicornis* (Fig. 4h, I; ESM Table S4). However, the percent of photosynthate translocated to the host did increase with temperature for *D. nummiforme* ($P < 0.0001$; Fig. 4g; ESM Table S4). When net photosynthesis was compared to symbiont density, a nonlinear trend was revealed with a noted exponential increase in photosynthesis as cell density declined (Fig. 5). With respect to linear trends between net photosynthesis and total translocation, *E. pallida* had the highest ratio of net photosynthesis:total translocation ($m = 4.52$), followed by the two scleractinian corals *M. hirsuta* ($m = 2.203$) and *P. damicornis* ($m = 2.155$; Fig. 5). Interestingly, the coral-limorph, *D. nummiforme* had the smallest ratio ($m = 1.283$) suggesting the largest amount of carbon assimilated within the host and not the symbiont.

Principal components analysis

A total of three principal components (PC) with eigenvalues of greater than 1 were extracted from our analysis of physiological variables (cellular density, chlorophyll, chlorophyll volume^{-1}, photosynthesis, translocation, percent translocation, ETR, σ_{PSII}, Fv/Fm, absorbance; Fig. 6). Physiological PC1 (eigenvalue = 4.95) explained 45 % of the variance, whereas PC2 (eigenvalue = 1.949) and PC3 (eigenvalue = 1.218) explained an additional 17.7 and 11 %, respectively. Host density, volume, percent translocation, σ_{PSII} and absorbance all had their highest loadings on PC1 and varied positively, whereas photosynthesis and Fv/Fm varied negatively (Table 4). Highest loadings for chlorophyll, chlorophyll volume^{-1} and ETR correlated positively with PC2.

Discussion

Previous work has suggested carbon limitation in some symbiont species (Weis 1993; Brading et al. 2011). From a photochemical perspective, greater availability of CO_2 through ocean acidification may alleviate such limitation by providing a greater sink through the photosynthetic electron transport chain and maintaining the plastoquinone pool in a more oxidized state. This may reduce potential heat stress to the PSII reaction center, a common site of thermal damage in thermally sensitive symbionts (Warner et al. 1999; Hill et al. 2011). For *Symbiodinium C3*, an increase in pCO_2 partially mitigated the thermal decline in Fv/Fm. Under ambient pCO_2 conditions, σ_{PSII} increased with temperature, increasing the light energy captured for photochemistry, and thus increasing the partial pressure over PSII and the potential for PSII degradation. However, elevated pCO_2 mitigated the thermal increase in σ_{PSII},

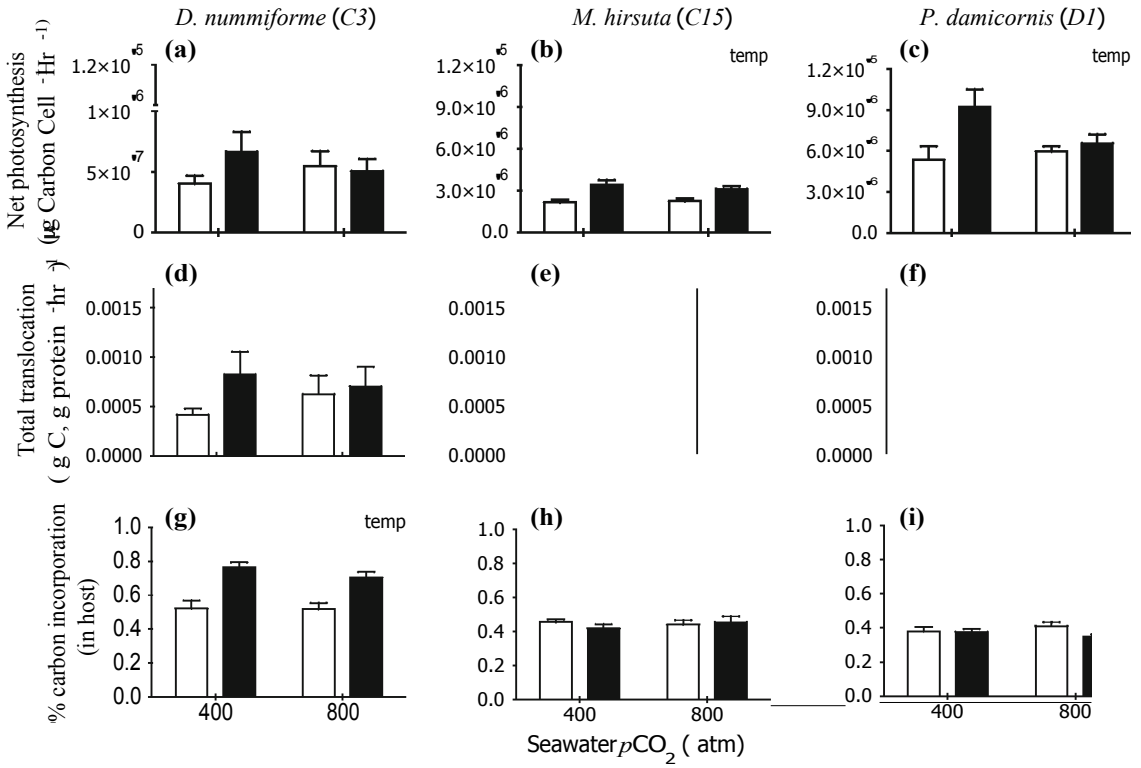

Fig. 4 Net photosynthesis, translocation and percent translocation for *Discosoma nummiforme* (a, d, g), *Montipora hirsuta* (b, e, h) and *Pocillopora damicornis* (c, f, i). Averages plus standard error ($n = 6$) are shown for two pCO_2 levels and two temperatures (26.5 °C: *open bars*, 32 °C: *dark bars*). The designation 'temp' indicates a significant temperature effect (two-way ANOVA)

thereby reducing the potential for reaction center degradation and allowed for thermal mitigation of Fv/Fm. This contrasts with the *D1* symbiont, where reductions in ETR were also observed, although both thermal and pCO_2 induced increases in maximum quantum yield. However, for the *D1* symbiont, r_{PSII} decreased with temperature, reducing the number of photons used for photosynthesis and decreasing ETR despite an increase in overall efficiency of PSII. Importantly, maximum quantum yields were relatively low within all species, consistent with yields observed in high-light acclimated symbionts (Robison and Warner 2006; Hennige et al. 2009). Likewise, Fv/Fm did not decrease over time within the control treatments (data not shown), which further substantiates the interpretation that these values reflect light acclimation as opposed to photoinactivation.

It is interesting to note that the thermal increase in net photosynthesis in the *D1* symbiont contrasted with a reduction in ETR. Major differences in the thermal response for these two metrics of photosynthetic activity suggest some decoupling between linear electron flow and downstream carbon utilization. For many classes of phytoplankton, as much as 60 % of gross photosynthesis can represent non-carbon assimilatory electron flow (Suggett et al. 2009; Halsey et al. 2013). In addition, a recent study showed photoreduction of oxygen to be a major alternative electron sink for cultured *Symbiodinium* during photosynthesis (Roberty et al. 2014). Hence, the reduction of ETR in the *D1* symbiont may reflect an alleviation of alternative electron flow and a greater use of reductant for carbon fixation in the Calvin cycle. In addition, the mitochondrial alternative oxidase (AOX) pathway may also be an important factor in this reduction of ETR, as AOX can account for 25–50 % of respiration in *Symbiodinium* and serve as a major electron sink (Oakley et al. 2014). A reduction in any or all of these pathways due to elevated temperature could explain the dichotomy between the reduction in PSII ETR and increased carbon incorporation observed here.

Along with PSII photochemical efficiency, reductions in symbiont number and chlorophyll concentration can indicate thermal or pCO_2 stress and/or acclimation (Grottoli et al. 2006; Kaniewska et al. 2012; Takahashi et al. 2013). A loss of symbionts is often thought to result from an increase in reactive oxygen species (ROS) produced by the symbionts under thermal stress (Suggett et al. 2008; Weis 2008; Baird et al. 2009). Although the photochemical evidence suggests that the *C3* symbiont was thermally sensitive while the *C15* and *D1* symbionts were more thermally tolerant, patterns in symbiont density did not

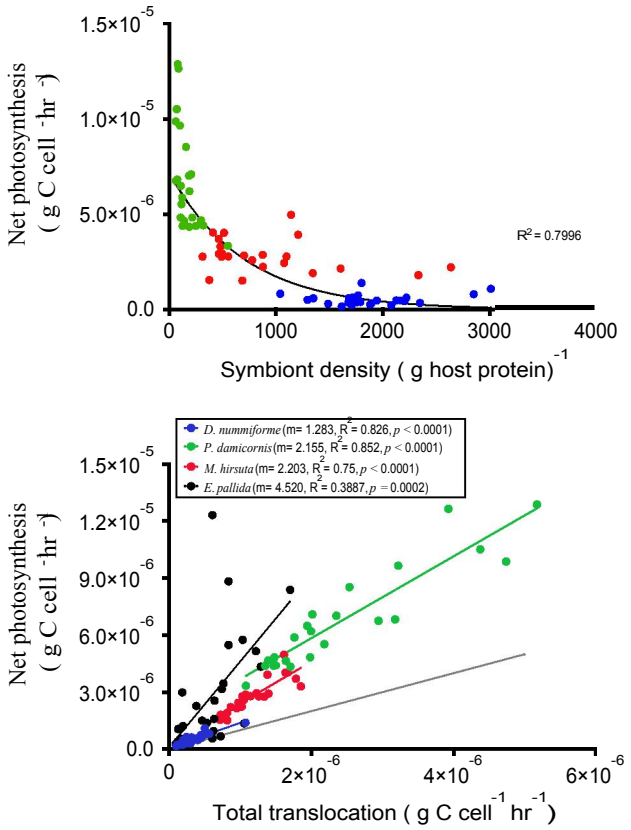

Fig. 5 Correlations between net photosynthesis and symbiont density (a) and net photosynthesis and total translocation (b). *Lines* represent the linear fit for *Discosoma nummiforme* (*blue*), *Pocillopora damicornis* (*green*), *Montipora hirsuta* (*red*) and *Exaiptasia pallida* (*black*). The *gray line* represents a P:T ratio of 1 when the rate of photosynthesis matches the rate of translocation to the host

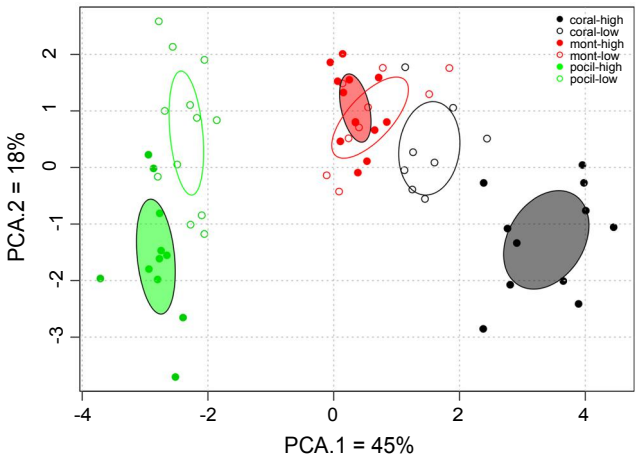

Fig. 6 Principal components analysis using all eleven physiological variables. Colors indicate species (*green*: *Pocillopora damicornis*, *red*: *Montipora hirsuta*, *black*: *Discosoma nummiforme*). *Open circles* indicate low-temperature treatments, and *closed circles* indicate high-temperature treatments. *Ellipses* represent a 99 % confidence bubble around the mean for low (*open ellipse*) and high (*closed ellipse*) temperature. Only temperature is represented as it explained the majority of significant differences among coral fragments

match this trend. *Discosoma nummiforme* maintained symbiont number, while both scleractinian species lost symbionts. As has been previously suggested (Hawkins et al. 2015; Krueger et al. 2015), increases in host ROS may have induced bleaching at high temperatures despite major evidence of thermal damage within the *D1* and *C15* symbionts. For *D. nummiforme*, greater host ROS scavenging and/or minimal increase in host ROS production may have allowed for stable symbiont cell numbers at high temperatures despite obvious signs of photostress in the *C3* symbiont. Nevertheless, reductions in cellular density and/or chlorophyll content are likely to impact the light environment for remaining cells.

For free-living phytoplankton, larger cell size tends to lead to smaller functional absorption cross sections, thereby reducing the susceptibility to photodamage from high-light stress (Finkel 2001; Key et al. 2010). This is typically due to a greater package effect as self-shading among chlorophyll molecules within the cell becomes more pronounced as cell size increases (Kirk 1994). Thermal reduction in chlorophyll *a* in the *C3* symbiont likely reduced the package effect, allowing for greater light capture per chlorophyll molecule. However, as previously mentioned, an increase in $\mathbf{r}_{PSII}$ only occurred within the ambient pCO_2 treatment, indicating a greater target for light harvesting and photochemistry at PSII under ambient pCO_2 conditions. The functional absorption cross section of PSII has been noted to both increase and decrease in free-living phytoplankton under high CO_2 which may be due to a reconfiguration of the light-harvesting antenna (Jin et al. 2013; Trimborn et al. 2014).

Despite a ca. 50 % reduction in cell density, absorbance within *M. hirsuta* increased with temperature. It is possible that this resulted from the slight increase in chlorophyll content and cellular volume, enabling better light capture within the symbiont. Alternatively, changes in the vertical distribution of remaining symbionts within the host tissue may also have influenced absorbance readings (Wangpraseurt et al. 2012). Changes in host fluorescent protein content may also have influenced the absorbance readings at elevated temperature. High-light acclimation increased fluorescence within the scleractinian coral *Galaxea fascicularis* (Ben-Zvi et al. 2014), and a similar increase in perceived light with a decrease in symbiont density within *M. hirsuta* may have triggered an increase in host fluorescent protein content, thereby increasing the absorbance under high temperature. An equally large (ca. 50 %) thermal reduction in cell density also occurred in *P. damicornis* in the ambient pCO_2 treatment. However, a loss in chlorophyll, along with an increase in cell size, resulted in major differences in intracellular chlorophyll density, largely influencing the light capture properties and the absorption spectra of this coral (Fig. 3c). These changes in

Table 4 Factor loadings for each variable within the principal components (PC) analysis

Variable	PC 1	PC 2	PC 3
Symbiont density	0.8587907		
Symbiont cellular volume	0.8508846		0.34858176
Chl a per cell	0.3342978	0.75811851	0.4413911
Chl a per $1 m^{-3}$	−0.417146	0.79116453	
Photosynthesis $cell^{-1}$	−0.8344981		
Total translocation	0.4939742	0.38862835	—0.25631065
Percent carbon incorporation	0.8148029		
Electron transport rate	—0.3861814	0.54240622	−0.27588867
Functional absorption cross section of PSII	0.6561665		−0.62267484
Fv/Fm	−0.760152		0.52984781
Absorbance at 675 nm	0.6608214	0.42105893	

Only significant ($P \setminus 0.05$) correlations are included. Values in bold indicate the axis of strongest loading for each physiological variable

absorption contrast with that of *D. nummiforme* where, despite a significant loss in cellular chlorophyll *a* with elevated temperature, the high symbiont density (normalized to animal protein) and absence of any change in cell volume led to minimal differences in colony absorbance. In addition, the lack of a highly reflective calcium carbonate skeleton and the greater tissue thickness may have further influenced this trend in *D. nummiforme*. Although further studies are needed to fully understand these bio-optical properties, it is clear that differences in morphology and light absorbance among anthozoan body types and cell physiologies can significantly influence the internal light field and productivity rates and likely further influence downstream processes important to host–algal symbioses.

Although major differences in net photosynthetic rates among symbiont types were apparent, no differences in translocation rate were observed among species or treatment conditions. Our results are similar to those observed for the coral *Stylophora pistillata*, where net photosynthesis and translocation rates were measured via ^{13}C isotopic analysis and did not change under high pCO_2 (Tremblay et al. 2013). However, Tremblay et al. (2013) noted that the percent of translocated photosynthate did increase with high pCO_2, whereas no change in percent translocation in *P. damicornis* or *M. hirsuta* in response to pCO_2 or temperature was noted here. Methodological differences may play a role in this comparison since the ^{14}C method cannot account for autotrophically fixed carbon that is then respired, which may cause an underestimation in photosynthetic rates and translocation (Tremblay et al. 2012). Likewise, the significantly higher pCO_2 concentration (3898 atm) used by Tremblay et al. (2013) may have played a role in this difference. Increased pCO_2 significantly increased productivity rates for several different anemone species (Suggett et al. 2012; Towanda and Thuesen 2012; Gibbin and Davy 2014); however, no changes in the percentage of photosynthate translocated to the host have been reported under elevated pCO_2.

Comparisons of productivity rates revealed a negative correlation between cell density and net photosynthesis (Fig. 5a). Additionally, increased photosynthesis with elevated temperature was only observed for the two scleractinians, where cell density also declined significantly, further strengthening the inverse relationship between productivity and cell density. A similar relationship was reported by Middlebrook et al. (2010) for *Acropora formosa* under thermal stress, where photosynthetic rates were measured via O_2 evolution. As previously mentioned, symbionts living in hospite are thought to be DIC limited (Weis 1993; Davy and Cook 2001; Wooldridge 2009). By reducing the cell density within the host, DIC availability may increase for the remaining symbionts, thus increasing the photosynthetic rate per cell. The two figures [Fig. 2c from Middlebrook et al. (2010) and Fig. 5a in this manuscript] show that this inverse relationship between photosynthesis and cell density exists both within the physiological constraints of a single species (Middlebrook et al. 2010) and as a ubiquitous response across multiple symbioses (Fig. 5a).

The physiological characteristics of each host–symbiont combination are critical for understanding the overall symbiosis and its unique acclimation strategy in response to environmental stress. The comparison between net maximal photosynthesis $algal\ cell^{-1}$ (P) and total carbon translocation $algal\ cell^{-1}$ (T; Fig. 5b) provides a simple yet useful ratio (P:T) comparison for assessing different symbionts in hospite. The slope and range of data provides a snapshot of one benefit of these symbioses, providing a

useful comparison among taxa as we attempt to better understand how climate change will influence different anthozoan–symbiont symbioses. Because the data reflect conditions under a range of physical stressors including controls, the resulting slopes for each species are indicative of each symbiosis across a physiological continuum. The greater slope of the relationship for *E. pallida* is indicative of symbionts translocating far less photosynthate to their host relative to their rate of carbon production, whereas the P:T ratio of *D. nummiforme* is much closer to unity and suggests that the *C3* symbiont shares a much larger percentage of the autotrophically fixed carbon with their host, regardless of the condition or applied stressor.

Overall, *P. damicornis* and *D. nummiforme* showed major changes in physiology in response to temperature, whereas little change was observed for *M. hirsuta* (Fig. 6). Differences in the biophysical and bio-optical properties along with carbon uptake and translocation form three clearly distinct host–symbiont combinations, each with a notably different response to thermal stress. The Cartesian distance among species within the PCA plot, along with the direction of change in response to elevated temperature, indicates major physiological differences in thermal stress mitigation or acclimation. Importantly, because fragments for each species were initially collected from a single colony, our results cannot be used to understand a population-wide response. Nevertheless, a large degree of physiological plasticity is still observed both within different fragments of the same colony and across the three coral species. Understanding how differences in physiological plasticity among coral species may influence the impact of future climate change on coral reef systems is an increasingly important topic. However, the unique acclimation strategies inherent to each host–symbiont combination require measurement of a broader spectrum of physiological variables to accurately characterize plasticity in response to environmental stress.

As noted for the *C1* and *D1* symbionts, similar thermal reductions in ETR can be brought about via vastly different photophysiological responses to elevated temperature and pCO_2. Additionally, reductions in PSII activity were not reflected within in overall carbon fixation which suggests that care must be taken when interpreting chlorophyll *a* fluorescence data alone. The inverse relationship between cell density and net photosynthesis corroborates previous work on carbon limitation and how it may apply during thermal bleaching events. Lastly, differences in the P:T ratios provide a unique metric with which to compare symbionts across different host–symbiont combinations. Future work will need to better focus on host–symbiont physiological diversity to better understand which cnidarian symbioses are more or less well poised to survive future climate change conditions.

References

Baird AH, Bhagooli R, Ralph P7, Takahashi S (2009) Coral bleaching: the role of the host. Trends Ecol Evol 24:16–20

Baker AC (2003) Flexibility and specificity in coral–algal symbiosis: diversity, ecology, and biogeography of *Symbiodinium*. Annu Rev Ecol Evol Syst 34:661–689

Ben-Zvi O, Eyal G, Loya Y (2014) Light-dependent fluorescence in the coral *Galaxea fascicularis*. Hydrobiologia 2014:1–12

Brading P, Warner ME, Davey P, Smith D7, Achterberg EP, Suggett D7 (2011) Differential effects of ocean acidification on growth and photosynthesis among phylotypes of *Symbiodinium* (Dinophyceae). Limnol Oceanogr 56:927–938

Brown B (1997) Coral bleaching: causes and consequences. Coral Reefs 16:129–138

Coffroth MA, Santos SR (2005) Genetic diversity of symbiotic dinoflagellates in the genus *Symbiodinium*. Protist 156:19–34

Comeau S, Edmunds P7, Spindel NB, Carpenter RC (2013) The responses of eight coral reef calcifiers to increasing partial pressure of CO_2 do not exhibit a tipping point. Limnol Oceanogr 589:388–398

Cooper TF, Ulstrup KE, Dandan SS, Heyward A7, Ku¨hl M, Muirhead A, O'Leary RA, Ziersen BEF, Van Oppen M7H (2011) Niche specialization of reef-building corals in the mesophotic zone: metabolic trade-offs between divergent *Symbiodinium* types. Proc R Soc Lond B Biol Sci 278:1840–1850

Davy SK, Cook C (2001) The relationship between nutritional status and carbon flux in the zooxanthellate sea anemone, *Aiptasia pallida*. Mar Biol 139:999–1005

Davy SK, Lucas IAN, Turner 7R (1996) Carbon budgets in temperate anthozoan–dinoflagellate symbioses. Mar Biol 126:773–783

Dudgeon SR, Aronson RB, Bruno 7F, Precht WF (2010) Phase shifts and stable states on coral reefs. Mar Ecol Prog Ser 413:201–216

Edmunds P7, Carpenter RC, Comeau S (2013) Understanding the threats of ocean acidification to coral reefs. Oceanography 26:149–152

Engebretson HP, Muller-Parker G (1999) Translocation of photosynthetic carbon from two algal symbionts to the sea anemone *Anthopleura elegantissima*. Biol Bull 197:72–81

Enriquez S, Mendez ER, Iglesias-Prieto R (2005) Multiple scattering on corals enhances light absorption by symbiotic algae. Limnol Oceanogr 50:1025–1032

Finkel ZV (2001) Light absorption and size scaling of light-limited metabolism in marine diatoms. Limnol Oceanogr 46:86–94

Fitt W (1985) Effect of different strains of the zooxanthella *Symbiodinium microadriaticum* on growth and survival of their coelenterate and molluscan hosts. Proc 5th Int Coral Reef Symp 6:131–136

Fitt W, Brown BE, Warner M, Dunne R (2001) Coral bleaching: interpretation of thermal tolerance limits and thermal thresholds in tropical corals. Coral Reefs 20:51–65

Gibbin EM, Davy SK (2014) The photo-physiological response of a model cnidarian–dinoflagellate symbiosis to CO_2-induced acidification at the cellular level. 7 Exp Mar Bio Ecol 457:1–7

Grottoli AG, Rodrigues L7, Palardy 7E (2006) Heterotrophic plasticity and resilience in bleached corals. Nature 440:1186–1189

Halsey KH, O'Malley RT, Graff 7R, Milligan A7, Behrenfeld M7 (2013) A common partitioning strategy for photosynthetic products in evolutionarily distinct phytoplankton species. New Phytol 198:1030–1038

Hawkins TD, Krueger T, Wilkinson SP, Fisher PL, Davy SK (2015) Antioxidant responses to heat and light stress differ with habitat in a common reef coral. Coral Reefs 34:1229–1241

Hennige S7, McGinley MP, Grottoli AG, Warner ME (2011) Photoinhibition of *Symbiodinium* spp. within the reef corals

Montastraea faveolata and *Porites astreoides*: implications for coral bleaching. Mar Biol 158:2515–2526

Hennige SJ, Suggett DJ, Warner ME, McDougall KE, Smith DJ (2009) Photobiology of *Symbiodinium* revisited: bio-physical and bio-optical signatures. Coral Reefs 28:179–195

Hill R, Brown CM, DeZeeuw K, Campbell DA, Ralph PJ (2011) Increased rate of D1 repair in coral symbionts during bleaching is insufficient to counter accelerated photo-inactivation. Limnol Oceangr 56:139–146

Hoadley KD, Rollison D, Pettay DT, Warner ME (2015) Differential carbon utilization and asexual reproduction under elevated pCO_2 conditions in the model anemone, *Exaiptasia pallida*, hosting different symbionts. Limnol Oceanogr 60:2108–2120

Hoegh-Guldberg O, Bruno JF (2010) The impact of climate change on the world's marine ecosystems. Science 328:1523–1528

Hoegh-Guldberg O, Mumby PJ, Hooten AJ, Steneck RS, Greenfield P, Gomez E, Harvell CD, Sale PF, Edwards AJ, Caldeira K, Knowlton N, Eakin CM, Iglesias-Prieto R, Muthiga N, Bradbury RH, Dubi A, Hatziolos ME (2007) Coral reefs under rapid climate change and ocean acidification. Science 318:1737–1742

Hughes TP, Connell JH (1999) Multiple stressors on coral reefs: a long-term perspective. Limnol Oceanogr 44:932–940

Hughes TP, Baird AH, Bellwood DR, Card M, Connolly SR, Folke C, Grosberg R, Hoegh-Guldberg O, Jackson JBC, Kleypas J, Lough JM, Marshall P, Nystrom M, Palumbi SR, Pandolfi JM, Rosen B, Roughgarden J (2003) Climate change, human impacts, and the resilience of coral reefs. Science 301:929–933

IPCC (2013) Summary for policymakers. In: Climate change 2013: the physical science basis. Contribution of Working Group I to the fifth assessment report of the Intergovernmental Panel on Climate Change. Cambridge University Press, Cambridge, UK and New York, NY, USA

Jin P, Gao K, Villafae VE, Campbell DA, Helbling EW (2013) Ocean acidification alters the photosynthetic responses of a coccolithophorid to fluctuating ultraviolet and visible radiation. Plant Physiol 162:2084–2094

Kaniewska P, Campbell PR, Kline DI, Rodriguez-Lanetty M, Miller DJ, Dove S, Hoegh-Guldberg O (2012) Major cellular and physiological impacts of ocean acidification on a reef building coral. PLoS One 7:e34659

Key T, McCarthy A, Campbell DA, Six C, Roy S, Finkel ZV (2010) Cell size trade-offs govern light exploitation strategies in marine phytoplankton. Environ Microbiol 12:95–104

Kirk JTO (1994) Light and photosynthesis in aquatic ecosystems. Cambridge University Press, Cambridge

Kitahara MV, Lin M-F, Foreˆt S, Huttley G, Miller DJ, Chen CA (2014) The "naked coral"hypothesis revisited—evidence for and against scleractinian monophyly. PLoS One 9:e94774

Kolber Z, Falkowski P (1998) Measurements of variable chlorophyll fluorescence using fast repetition rate techniques: defining methodology and experimental protocols. Biochim Biophys 1367:88–107

Krueger T, Hawkins TD, Becker S, Pontasch S, Dove S, Hoegh-Guldberg O, Leggat W, Fisher PL, Davy SK (2015) Differential coral bleaching—contrasting the activity and response of enzymatic antioxidants in symbiotic partners under thermal stress. Comp Biochem Physiol A Mol Integr Physiol 190:15–25

Kuguru B, Achituv Y, Gruber DF, Tchernov D (2010) Photoacclimation mechanisms of corallimorpharians on coral reefs: photosynthetic parameters of zooxanthellae and host cellular responses to variation in irradiance. J Exp Mar Bio Ecol 394:53–62

LaJeunesse TC (2001) Investigating the biodiversity, ecology, and phylogeny of endosymbiotic dinoflagellates in the genus *Symbiodinium* using the ITS region: in search of a "species"level marker. J Phycol 37:866–880

LaJeunesse TC, Loh WKW, van Woesik R, Hoegh-Guldberg O, Schmidt GW, Fitt WK (2003) Low symbiont diversity in southern Great Barrier Reef corals, relative to those of the Caribbean. Limnol Oceanogr 48:2046–2054

Leal MC, Hoadley K, Pettay DT, Grajales A, Calado R, Warner ME (2015) Symbiont type influences trophic plasticity of a model cnidarian–dinoflagellate symbiosis. J Exp Biol 218:858–863

Lewis E, Wallace D (1998) Program developed for CO_2 system calculations. Carbon Dioxide Information Analysis Center, Oak Ridge National Laboratory, Oak Ridge, TN, USA

Medina M, Collins AG, Takaoka TL, Kuehl JV, Boore JL (2006) Naked corals: skeleton loss in Scleractinia. Proc Natl Acad Sci U S A 103:9096–9100

Middlebrook R, Anthony KR, Hoegh-Guldberg O, Dove S (2010) Heating rate and symbiont productivity are key factors determining thermal stress in the reef-building coral *Acropora formosa*. J Exp Biol 213:1026–1034

Norstro¨m AV, Nystro¨m M, Lokrantz J, Folke C (2009) Alternative states on coral reefs: beyond coral–macroalgal phase shifts. Mar Ecol Prog Ser 376:295–306

Oakley CA, Hopkinson BM, Schmidt GW (2014) Mitochondrial terminal alternative oxidase and its enhancement by thermal stress in the coral symbiont *Symbiodinium*. Coral Reefs 33:543–552

Porra RJ, Thompson WA, Kriedemann PE (1989) Determination of accurate extinction coefficients and simultaneous equations for assaying chlorophylls *a* and *b* extracted with four different solvents: verification of the concentration of chlorophyll standards by atomic absorption spectroscopy. Biochim Biophys Acta 975:384–394

Roberty S, Berne N, Bailleul B, Cardol P (2014) PSI Mehler reaction is the main alternative photosynthetic electron pathway in *Symbiodinium* sp., symbiotic dinoflagellates of cnidarians. New Phytol 204:81–91

Robison JD, Warner ME (2006) Differential impacts of photoacclimation and thermal stress on the photobiology of four different phylotypes of *Symbiodinium* (Pyrrhophyta). J Phycol 42:568–579

Rodriguez-Roma´n A, Herna´ndez-Pech X, Thome´ PE, Enriquez S, Iglesias-Prieto R (2006) Photosynthesis and light utilization in the Caribbean coral *Montastraea faveolata* recovering from a bleaching event. Limnol Oceanogr 51:2702–2710

Schoepf V, Grottoli AG, Warner ME, Cai WJ, Melman TF, Hoadley KD, Pettay DT, Hu X, Li Q, Xu H, Wang Y, Matsui Y, Baumann JH (2013) Coral energy reserves and calcification in a high-CO_2 world at two temperatures. PLoS One 8:e75049

Shick JM, Dowse HB (1985) Genetic basis of physiological variation in natural populations of sea anemones: Intra-and interclonal analyses of variance. In: Gibbs PE (ed) Proceedings of the 19th European Marine Biology Symposium, Plymouth, Devon, UK, 16–21 September 1984. Cambridge University Press, Cambridge, UK

Shick JM, Iglic K, Wells ML, Trick CG, Doyle J, Dunlap WC (2011) Responses to iron limitation in two colonies of *Stylophora pistillata* exposed to high temperature: implications for coral bleaching. Limnol Oceangr 56:813–828

Suggett DJ, MacIntyre HL, Kana TM, Geider RJ (2009) Comparing electron transport with gas exchange: parameterising exchange rates between alternative photosynthetic currencies for eukaryotic phytoplankton. Aquat Microb Ecol 56:147–162

Suggett DJ, Oxborough K, Baker NR, MacIntyre HL, Kana TM, Geider RJ (2003) Fast repetition rate and pulse amplitude modulation chlorophyll a fluorescence measurements for assessment of photosynthetic electron transport in marine phytoplankton. Eur J Phycol 38:371–384

Suggett DJ, Warner ME, Smith DJ, Davey P, Hennige S, Baker NR (2008) Photosynthesis and production of hydrogen peroxide by

Symbiodinium (Pyrrhophyta) phylotypes with different thermal tolerances. J Phycol 44:948–956

Suggett DJ, Hall-Spencer JM, Rodolfo-Metalpa R, Boatman TG, Payton R, Tye Pettay D, Johnson VR, Warner ME, Lawson T (2012) Sea anemones may thrive in a high CO_2 world. Glob Chang Biol 18:3015–3025

Takahashi S, Yoshioka-Nishimura M, Nanba D, Badger MR (2013) Thermal acclimation of the symbiotic alga *Symbiodinium* spp. alleviates photobleaching under heat stress. Plant Physiol 161:477–485

Tkachenko KS, Wu B-J, Fang L-S, Fan T-Y (2007) Dynamics of a coral reef community after mass mortality of branching *Acropora* corals and an outbreak of anemones. Mar Biol 151:185–194

Towanda T, Thuesen EV (2012) Prolonged exposure to elevated CO_2 promotes growth of the algal symbiont *Symbiodinium muscatinei* in the intertidal sea anemone *Anthopleura elegantissima*. Open Biol 1:615–621

Tremblay P, Fine M, Maguer JF, Grover R (2013) Ocean acidification increases photosynthate translocation in a coral–dinoflagellates symbiosis. Biogeosciences 10:83–109

Tremblay P, Grover R, Maguer JF, Legendre L, Ferrier-Page`s C (2012) Autotrophic carbon budget in coral tissue: a new 13C-based model of photosynthate translocation. J Exp Biol 215:1384–1393

Trimborn S, Thoms S, Petrou K, Kranz SA, Rost B (2014) Photophysiological responses of Southern Ocean phytoplankton to changes in CO_2 concentrations: short-term versus acclimation effects. J Exp Mar Bio Ecol 451:44–54

Wangpraseurt D, Larkum AWD, Ralph PJ, Kuhl M (2012) Light gradients and optical microniches in coral tissues. Front Microbiol 3:316

Warner M, Fitt W, Schmidt G (1996) The effects of elevated temperature on the photosynthetic efficiency of zooxanthellae *in hospite* from four different species of reef coral: a novel approach. Plant Cell Environ 19:291–299

Warner M, Fitt W, Schmidt G (1999) Damage to photosystem II in symbiotic dinoflagellates: a determinant of coral bleaching. Proc Natl Acad Sci U S A 96:8007–8012

Weis VM (1993) Effect of dissolved inorganic carbon concentration on the photosynthesis of the symbiotic sea anemone *Aiptasia pulchella* Carlgren: role of carbonic anhydrase. J Exp Mar Bio Ecol 174:209–225

Weis VM (2008) Cellular mechanisms of cnidarian bleaching: stress causes the collapse of symbiosis. J Exp Biol 211:3059–3066

Weisz JB, Massaro AJ, Ramsby BD, Hill MS (2010) Zooxanthellar symbionts shape host sponge trophic status through translocation of carbon. Biol Bull 219:189–197

Wooldridge SA (2009) A new conceptual model for the enhanced release of mucus in symbiotic reef corals during 'bleaching' conditions. Mar Ecol Prog Ser 396:145–152

Yao W, Byrne RH (1998) Simplified seawater alkalinity analysis: use of linear array spectrometers. Deep Sea Res Part I Oceanogr Res Pap 45:1383–1392